Pol. J. Environ. Stud. Vol. XX, No. X (XXXX), 1-14
DOI: *10.15244/pjoes/221896* ONLINE PUBLICATION DATE: 2026-09-29

Original Research

Biosynthesized Nano-Selenium Improves Selenium Biofortification, Soil Microbial Functions, and Nutrient Cycling in Paddy Ecosystems

Peifeng Xu[1, 2#], Xiaorong Zhang[1#], Zongqiang Gong[1]*, Boshi Wang[3], Meng Yuan[3], Yanjie Jia[1], Shuhai Guo[4]

[1]CAS Key Laboratory of Forest Ecology and Silviculture, Institute of Applied Ecology, Chinese Academy of Sciences, Shenyang 110016, PR China
[2]University of Chinese Academy of Sciences, Beijing, 100049, PR China
[3]School of Municipal and Environmental Engineering, Shenyang Jianzhu University, Shenyang 110168, PR China
[4]National-Local Joint Engineering Laboratory of Contaminated Soil Remediation by Bio-physicochemical Synergistic Process, Institute of Applied Ecology, Chinese Academy of Sciences, Shenyang 110016, PR China

Received: 13 November 2025
Accepted: 15 May 2026

Abstract

Nano-selenium (nano-Se) fertilizers are emerging as a promising strategy to alleviate selenium (Se) deficiency in rice-producing regions, where Se deficiency affects nearly one billion people globally. However, their impacts on Se bioavailability, rhizosphere microbial ecology, and nutrient cycling in flooded paddy soils remain poorly understood. In this study, a field experiment was conducted to evaluate biologically synthesized nano-Se (BSeNP) and chemically synthesized nano-Se (CSeNP) in terms of Se uptake, soil–plant Se dynamics, and microbial community responses in a rice system. Both nano-Se treatments significantly enhanced Se accumulation in stems, leaves, and grains. BSeNP induced stronger Se enrichment in vegetative tissues, whereas both treatments achieved comparable increases in grain Se content relative to the control. Soil Se decreased gradually during plant growth while plant Se increased, reflecting efficient nano-Se dissolution, sustained rhizosphere availability, and effective root-to-shoot translocation.

High-throughput 16S rRNA gene sequencing revealed substantial microbial restructuring, characterized by increased abundance of Proteobacteria and enrichment of Se-transforming genera, including *Burkholderia*, *Rhodobacter*, and *Sphingomonas*. Co-occurrence network and functional-prediction analyses indicated enhanced nitrogen and sulfur cycling pathways, increased ABC transporter activity, and elevated microbial metabolic and redox functions, particularly under BSeNP. Correlation analyses demonstrated strong coupling between plant Se accumulation, soil nutrients, and microbial functional traits, highlighting coordinated plant–soil–microbe interactions.

# equal contribution
*e-mail: zgong@iae.ac.cn
0000-0002-5646-6227

Collectively, biosynthesized nano-Se exhibited superior biofortification potential and ecological compatibility compared with chemically synthesized forms, providing a bio-based and sustainable approach for improving Se nutrition and soil microbial function in paddy agroecosystems.

Keywords: biosynthesized nano-selenium, selenium biofortification, soil microbial functions, nutrient cycling, paddy ecosystems

Introduction

Selenium (Se) is an essential micronutrient for humans and animals, playing important roles in antioxidant defense, immune regulation, and redox homeostasis [1]. However, Se deficiency remains widespread in many parts of the world, including Northeast Asia and parts of Europe, resulting in inadequate dietary Se intake and increased risks of metabolic and immune disorders [2]. Agronomic biofortification is therefore regarded as an effective strategy for increasing Se concentrations in staple crops such as rice, thereby improving dietary Se intake and public health [3]. Nevertheless, conventional Se fertilizers, such as sodium selenite and selenate, often show low utilization efficiency and may pose environmental risks because of leaching, volatilization, and redox transformation in soil systems [4].

Nanotechnology has emerged as a promising approach for nutrient delivery, owing to its controlled release behavior, enhanced uptake efficiency, and reduced toxicity risk compared with bulk or ionic forms [5]. Among these materials, selenium nanoparticles (SeNPs) have attracted particular attention because of their considerable agronomic potential. Previous studies have shown that SeNPs can improve photosynthetic performance, enhance antioxidant capacity, and increase micronutrient accumulation in rice and vegetable crops [6, 7]. However, most of these studies have been conducted under greenhouse or hydroponic conditions, and field-based evidence regarding the fertilization efficiency, environmental behavior, and ecological safety of nano-selenium remains limited [8].

In paddy ecosystems, soil microbial communities play important roles in regulating Se transformation through reduction, oxidation, methylation, and organic-binding processes [9, 10]. They also participate in nitrogen and sulfur cycling, thereby affecting plant nutrient availability and overall soil health [11]. At the same time, increasing evidence suggests that nanomaterials can reshape microbial assemblages, alter ecological networks, and modulate microbial functional traits in agroecosystems [12]. Therefore, understanding how nano-selenium interacts with rhizosphere microbiota is essential for evaluating its agricultural applicability and ecological sustainability [13].

Compared with chemically synthesized nanoparticles, biogenic nanoparticles derived from microbes or plant extracts often possess greater biocompatibility, improved stability, and more diverse surface functionalization, which may support safer and more favorable interactions with soil microbial communities [14, 15]. Despite these potential advantages, comparative field-scale studies directly evaluating biosynthesized SeNPs (BSeNP) and chemically synthesized SeNPs (CSeNP) in rice production systems remain scarce, especially in relation to their effects on Se biofortification, microbial community assembly, and nutrient-cycling functions.

To address these knowledge gaps, the present study compared BSeNP and CSeNP in a field rice system and evaluated their effects on Se uptake, translocation, and biofortification efficiency. In addition, we investigated changes in rhizosphere microbial community composition, co-occurrence patterns, and predicted functional pathways under nano-selenium fertilization. By integrating plant, soil, and microbial responses, this study provides new insights into soil–plant–microbe interactions under nano-enabled fertilization and offers a scientific basis for the sustainable use of Se fertilizers in paddy agroecosystems.

Materials and Methods

Study Site Description

The field experiment was conducted in an agricultural area of Zhenlai County, Baicheng City, Jilin Province, China. The soil had a sandy loam texture, with a pH of 8.42±0.20 and an electrical conductivity of 1.68 dS m^{-1} (1:5 soil/water). Initial soil properties included total organic carbon of 1.2% (w/w), total nitrogen of 0.1% (w/w), and available potassium of 370.46 mg kg^{-1}, indicating suitable conditions for rice cultivation. The region has a temperate continental climate, with an average annual temperature of 5.5-6.5ºC. During the rice-growing season (May-September), mean air temperature ranged from 22 to 25ºC, and precipitation averaged 500-700 mm (Fig. 1).

Preparation of Experimental Fertilizers

Control Group (CK)

The control group (CK) received standard NPK fertilization: 220 kg ha^{-1} nitrogen (N) as urea, 110 kg ha^{-1} phosphorus (P) as diammonium phosphate, and 110 kg ha^{-1} potassium (K) as potassium sulfate. Fertilizers were applied in two stages: 60% as basal application two days before transplanting and 40%

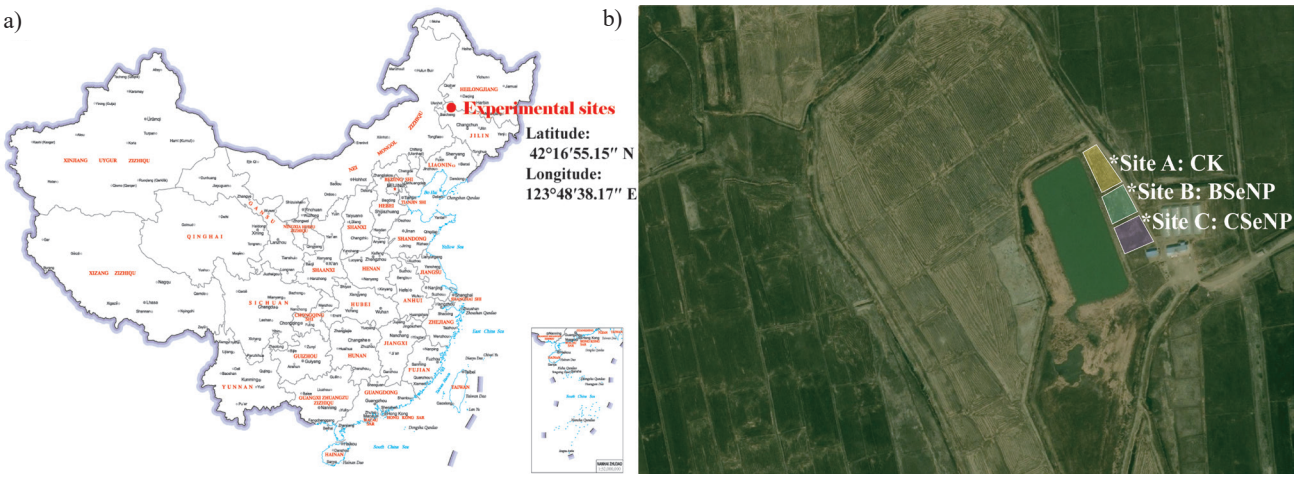

Fig. 1. Field site and experimental design. a) Geographic location of the rice field experimental site in Northeast China, including coordinates. b) Layout and spatial distribution of treatment plots: CK (control), BSeNP (biosynthesized nano-selenium), and CSeNP (chemically synthesized nano-selenium). All plots were managed under identical agronomic conditions.

as topdressing 10 days after transplanting. No selenium fertilizer was applied in CK.

Biosynthesized Selenium Nanofertilizer (BSeNP)

Biosynthesized selenium nanoparticles (BSeNPs) were prepared using fresh mandarin extract as a natural reducing and stabilizing agent. Briefly, 20 mL of citrus extract, 0.4 g sodium selenite (Na_2SeO_3), and 1.5 g glucose were mixed in a sterile flask. The pH was adjusted to 7.0±0.1, and the solution was incubated at 70ºC for 3 h in the dark with constant shaking (200 rpm), followed by incubation at 37ºC for 72 h. Formation of BSeNPs was visually confirmed by a color change from pale yellow to red.

Chemically Synthesized Selenium Nanofertilizer (CSeNP)

Chemically synthesized SeNPs (CSeNPs) were obtained by reducing Na_2SeO_3 (0.4 g) with glucose (1.5 g) and ascorbic acid (1.6 g) in the presence of alkyl polyglucoside (1.6 g) as a stabilizer. The reaction mixture was ultrasonicated (40 kHz, 60 W) for 30 min and maintained at room temperature until a stable reddish suspension formed. Compared with BSeNPs, CSeNPs were chemically reduced and lacked the biologically mediated color transition observed during BSeNP synthesis.

Physicochemical Characterization of BSeNP and CSeNP

The particle size distribution and colloidal stability of BSeNP and CSeNP were measured using dynamic light scattering (DLS) and zeta potential analysis. Measurements were conducted with a Malvern particle size analyzer at 25ºC, using a scattering angle of 90º and a refractive index of 1.59. Each sample was measured in triplicate.

The surface morphology and aggregation of the nanoparticles were examined by scanning electron microscopy (SEM). Prior to imaging, samples were freeze-dried to preserve particle structure and facilitate comparison of particle size, shape, and aggregation characteristics between formulations.

Surface functional groups were analyzed by Fourier transform infrared spectroscopy (FTIR). Freeze-dried nanoselenium samples were mixed with spectrographic-grade KBr, ground, and pressed into pellets. Spectra were recorded over the range of 4000-400 cm^{-1} to identify characteristic chemical bonds and functional groups.

Experimental Design and Treatments

The field experiment included three treatments: CK (control), BSeNP, and CSeNP. The BSeNP and CSeNP treatments were applied as foliar sprays by diluting 250 mL of fertilizer stock in 30 L of deionized water at the heading and early filling stages. The final Se concentration in the foliar spray solution was approximately 0.167 g L^{-1}. The field application rate was set at 37.5 g Se ha^{-1}, based on a prior pot optimization experiment in which this concentration produced the most favorable seedling growth performance among the tested treatments.

Each treatment was arranged in a randomized complete block design with three replicates. Prior to transplanting, the soil was tilled to a depth of 0.2 m and homogenized using a rotary tiller. Before fertilizer application, three composite soil samples were collected from each plot using a five-point sampling method to determine baseline soil physicochemical properties.

Sample Collection and Processing

Soil and plant samples were collected at three key growth stages: T_0 (Tillering, 15 days after the first fertilizer application), T_1 (Grain Filling, 15 days after the second fertilizer application), and T_2 (Maturity, at full ripening).

At each stage, five composite soil samples were collected from each plot using a five-point sampling method. Each composite sample (~1 kg) consisted of soil cores from 0-20 cm depth and was transported to the laboratory at 4ºC. Samples were then subdivided into two subsamples: one stored at 4ºC for physicochemical analysis and the other stored at −80ºC for microbial community analysis via 16S rRNA sequencing.

Prior to analysis, all soil samples were passed through a 100-mesh (0.15 mm) nylon sieve to remove plant debris and stones. Rice plants were harvested simultaneously, and roots, stems, and leaves were separated for physiological assays and selenium content determination.

Analytical Methods

Determination of Selenium in Rice Tissues and Grain

Dried roots, stems, leaves, and grains were ground into fine powder and passed through a 0.5 mm sieve. For selenium analysis, 0.5 g of each sample was digested with 5 mL concentrated HNO_3 (69%) and 2 mL $HClO_4$ (70%) on a clean bench. After cooling, the digest was transferred to a 50 mL volumetric flask and diluted to volume with deionized water. Selenium concentrations were measured using a hydride generation atomic fluorescence spectrometer (AFS-933, Beijing Titan Instrument Co., Ltd., China).

Determination of Soil Physicochemical Properties

Soil pH was determined in a 1:2.5 (w/v) soil-water suspension using a calibrated pH meter (PHS-3C, INESA Scientific Instrument Co., Ltd., Shanghai, China). Electrical conductivity (EC) was measured in a 1:5 (w/v) soil-water suspension using a conductivity meter (DDS-307, Leici Electrical Appliance Co., Ltd., China). Suspensions were shaken for 30 min at 180 rpm and allowed to settle for 15 min prior to measurement.

Total organic carbon (TOC) was measured using the potassium dichromate oxidation method [16]. Briefly, 0.5 g of air-dried soil was digested with 5 mL 1 M $K_2Cr_2O_7$ and 7.5 mL H_2SO_4 at 180ºC for 30 min, diluted to 50 mL, and absorbance was recorded at 590 nm.

Ammonium nitrogen (NH_4^+) was extracted with 2 M KCl and analyzed colorimetrically with Nessler's reagent at 420 nm. Available potassium (AK) was extracted with 1 M NH_4OAc and measured by flame photometry. Soil nitrate nitrogen (NO_3^-) was extracted and measured spectrophotometrically at 220 nm.

Chlorophyll Content in Leaves

Fresh rice leaves (0.1 g) were cut into small pieces and immersed in 10 mL of pre-chilled extraction solution (acetone:absolute ethanol:distilled water, 4.5:4.5:1, v/v/v) in 15 mL centrifuge tubes, wrapped in aluminum foil, and incubated at 4ºC for 24 h. Chlorophyll contents were calculated from the absorbance of the supernatant measured at 663 and 645 nm using a spectrophotometer.

Superoxide Dismutase (SOD) Activity

SOD activity was determined using a commercial assay kit (Solarbio, Beijing, China) based on the inhibition of nitroblue tetrazolium (NBT) photochemical reduction. Approximately 0.5 g of fresh leaf tissue was homogenized in 5 mL 50 mM phosphate buffer (pH 7.8), centrifuged at 10,000×g for 15 min at 4ºC, and enzyme activity was measured in the supernatant. Results were expressed as U g^{-1} fresh weight (FW).

Malondialdehyde (MDA) Content

MDA content was determined using a commercial kit (Solarbio, Beijing, China) via the thiobarbituric acid (TBA) reaction. Briefly, 0.5 g of fresh leaf tissue was homogenized in 5 mL 0.1% (w/v) trichloroacetic acid (TCA), centrifuged at 10,000×g for 15 min at 4ºC, and the supernatant was used for MDA measurement. Absorbance was read at 532 nm, and MDA content was expressed as nmol g^{-1} FW.

16S rRNA Gene Sequencing and Bioinformatics Analysis

Soil microbial community profiling was conducted by sequencing the V3–V4 hypervariable region of the bacterial 16S rRNA gene using the Illumina MiSeq platform (Illumina, San Diego, CA, USA). Total genomic DNA was extracted from 0.5 g of soil per sample using the DNeasy PowerSoil Kit (Qiagen, Germany) following the manufacturer's protocol.

PCR amplification was performed with primers 338F (5′-ACTCCTACGGGAGGCAGCAG-3′) and 806R (5′-GGACTACHVGGGTWTCTAAT-3′). The PCR program consisted of initial denaturation at 95ºC for 3 min, followed by 27 cycles of 95ºC for 30 s, 55ºC for 30 s, and 72ºC for 30 s, with a final extension at 72ºC for 10 min. Amplicons were purified, quantified, and pooled for paired-end sequencing (2 × 300 bp) using the MiSeq Reagent Kit v3 (600-cycle).

Raw sequencing reads were processed using QIIME2 (version 2022.2). Quality filtering, denoising, and chimera removal were conducted using the DADA2 algorithm. Representative amplicon sequence variants (ASVs) were taxonomically assigned based on the SILVA 138 database.

Downstream analyses were performed in R (version 4.2.2). Alpha-diversity and beta-diversity metrics were

calculated using the vegan package. Principal coordinate analysis (PCoA) was used to visualize overall community differences. Co-occurrence networks were constructed based on Spearman correlations ($r>0.8$, $p<0.05$) using igraph, and visualized with ggplot2. Redundancy analysis (RDA) and Mantel tests were performed with vegan to assess relationships between microbial communities and environmental variables. Heatmaps of taxonomic and functional profiles were generated using pheatmap (v1.0.12). Functional prediction of microbial communities was performed using KEGG databases, with ecological functions further annotated via microeco.

Results

Physicochemical Characterization of BSeNP and CSeNP

Dynamic light scattering (DLS) analysis revealed distinct differences in particle-size distribution between BSeNP and CSeNP (Fig. 2a) and b)). BSeNP exhibited an average hydrodynamic diameter of 48.48 nm and a zeta potential of −34.3 mV, whereas CSeNP showed a larger average diameter of 86.63 nm with a zeta potential of −27.5 mV. The DLS profiles further indicated that BSeNP had a broader particle-size distribution, while CSeNP particles were more narrowly dispersed. Among the chemically synthesized formulations, CSeNP displayed an almost Gaussian size-distribution pattern with a low polydispersity index (PDI, 0.057±0.007), suggesting a relatively monodisperse population.

Scanning electron microscopy (SEM) observations were generally consistent with the DLS results (Fig. 2c) and d)). CSeNP particles were distributed more uniformly on the stabilizer matrix, with relatively consistent particle size and limited aggregation, and most particles were within the range of 40-100 nm. In contrast, BSeNP exhibited a wider size range and less uniform distribution. Comparative SEM observations also suggested that several non-CA formulations showed more pronounced aggregation and irregular morphology, whereas CSeNP maintained a relatively dispersed particulate structure.

Fourier transform infrared (FTIR) spectra revealed clear differences in surface chemical characteristics among the formulations (Fig. 2e)). All SeNP formulations displayed absorption bands in the 2920-2925 cm^{-1} region, corresponding to the asymmetric stretching vibration of aliphatic $–CH_2$ groups. Carbonyl-related vibrations were observed in the 1590-1630 cm^{-1} region, while polysaccharide-associated C–O–C/C–O–H vibrations appeared near 1032 cm^{-1}. Notably, the –OH absorption band of CSeNP showed a red shift of approximately 28.7 cm^{-1}, and the polysaccharide-related band exhibited a characteristic peak at 620.93 cm^{-1}. These spectral differences indicate distinct surface functional-group environments among the formulations, reflecting differences in synthesis route and surface chemistry.

Effects of Nano-Selenium on Rice Physiological Performance

The application of nano-selenium was accompanied by pronounced changes in several key physiological indicators of rice, providing insight into the potential mechanisms underlying the growth-promoting effects of nano-selenium (Fig. 3). Both BSeNP and CSeNP significantly increased superoxide dismutase (SOD) activity during the grain-filling stage (Fig. 3a)), indicating an enhanced antioxidative response in treated plants. Compared with CK, rice plants receiving nano-selenium exhibited stronger enzymatic antioxidant capacity, with BSeNP generally showing a greater stimulatory effect than CSeNP.

This strengthened antioxidant response was also reflected in malondialdehyde (MDA) content (Fig. 3b)). Both nano-selenium treatments reduced MDA accumulation during the filling stage, suggesting alleviation of membrane lipid peroxidation and oxidative damage. The decrease in MDA was more pronounced under BSeNP treatment, indicating that biosynthesized nano-selenium may provide a stronger protective effect against oxidative stress than the chemically synthesized counterpart.

In addition to antioxidant-related indicators, nano-selenium also improved photosynthetic performance, as reflected by chlorophyll content (Fig. 3c)). Rice plants treated with BSeNP and CSeNP exhibited higher chlorophyll concentrations during the grain-filling period than CK, indicating enhanced maintenance of photosynthetic pigment status during this critical reproductive stage. Taken together, the increases in SOD activity and chlorophyll content, coupled with the reduction in MDA, suggest that nano-selenium treatments improved the physiological status of rice plants and may have contributed to better Se assimilation and biomass development.

Selenium Dynamics in the Rice-Soil System

The temporal variation of selenium (Se) concentrations in rice tissues revealed clear differences in uptake and translocation patterns under nano-selenium treatments (Fig. 4(a-c)). Both BSeNP and CSeNP enhanced Se accumulation in rice tissues relative to CK, but the magnitude of the response varied among tissues and growth stages. In stems and leaves, Se concentrations increased progressively following nano-selenium application, indicating active uptake and internal transport during plant development. The increase was consistently more pronounced in BSeNP-treated plants, suggesting a stronger capacity to facilitate Se entry and redistribution within the plant system.

At maturity, BSeNP resulted in the highest Se accumulation in all plant organs. Grain Se concentration

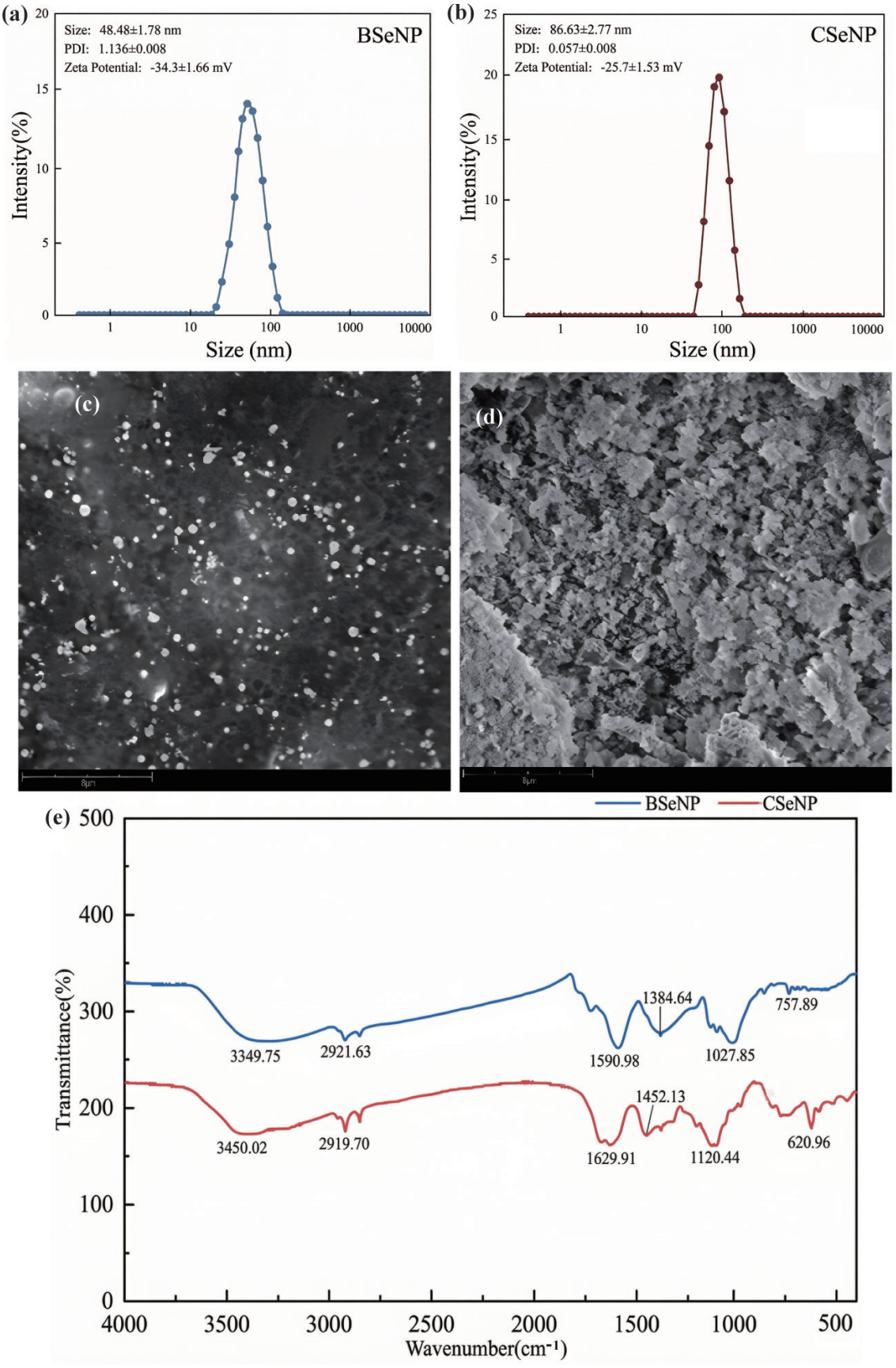

Fig. 2. Physicochemical characterization of biosynthesized and chemically synthesized nano-selenium. (a-b) Particle size distribution of biosynthesized nano-selenium (BSeNP) and chemically synthesized nano-selenium (CSeNP), determined by dynamic light scattering (DLS), including particle size, polydispersity index (PDI), and zeta potential. (c-d) Scanning electron microscopy (SEM) images of BSeNP and CSeNP, showing differences in particle morphology and aggregation characteristics. e) Fourier transform infrared (FTIR) spectra of BSeNP and CSeNP, indicating variations in surface functional groups and chemical bonding environments.

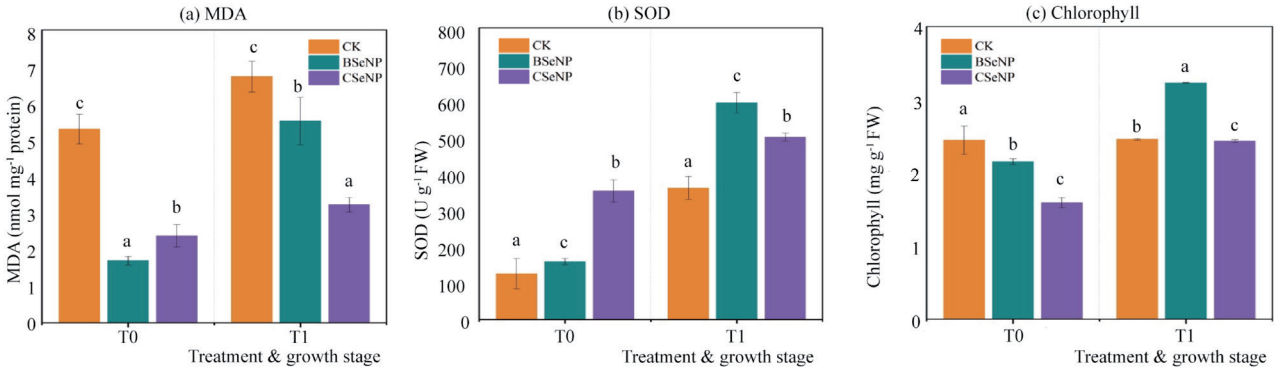

Fig. 3. Effects of nano-selenium on key physiological indicators of rice. a) Malondialdehyde (MDA) content, b) superoxide dismutase (SOD) activity, and c) chlorophyll concentration measured at tillering (T0) and grain-filling (T1) stages under CK, BSeNP, and CSeNP treatments. Error bars represent mean±SD (n = 3). Different letters indicate significant differences among treatments at each stage ($p<0.05$, one-way ANOVA followed by Tukey's HSD test).

increased by 263% relative to CK, whereas CSeNP produced a 247% increase (Fig. 4c)), indicating that both nano-selenium treatments effectively improved Se biofortification but that BSeNP generally exerted the stronger effect. The difference between BSeNP and CSeNP was particularly evident in vegetative tissues, where the response in leaves was stronger than that observed in grains, consistent with the foliar-application pathway and subsequent redistribution of Se during grain filling.

These results suggest that nano-selenium fertilizers, particularly BSeNP, improved Se bioavailability and plant uptake efficiency compared with conventional fertilization. The smaller particle size and higher surface reactivity of nano-Se may have facilitated closer contact with leaf and root surfaces, thereby enhancing ion exchange, assimilation, and translocation. Overall, nano-Se application accelerated the transformation and cycling of Se between soil and plant compartments and promoted more efficient transfer of Se into edible tissues, supporting its value for agronomic Se biofortification in rice-based systems.

Microbial Community Composition and Structure under Different Selenium Treatments

Nano-selenium application markedly influenced soil microbial diversity and community composition in paddy soil. Principal coordinates analysis (PCoA) based on Bray–Curtis dissimilarity showed clear separation between CK and the nano-selenium-treated groups along the first principal axis, which explained >25% of the total variance (Fig. 5a)). This pattern indicates that both BSeNP and CSeNP substantially altered the microbial assemblage relative to the untreated control, with BSeNP producing the strongest shift in community structure.

Redundancy analysis (RDA) further demonstrated that total carbon (TC), total nitrogen (TN), and available potassium (AK) were the main environmental variables associated with these compositional changes (Fig. 5b)). Samples from BSeNP-treated plots clustered positively with TC and AK, suggesting that nano-selenium application, particularly BSeNP, was associated with shifts in nutrient-related environmental conditions that may have contributed to restructuring of the rhizosphere

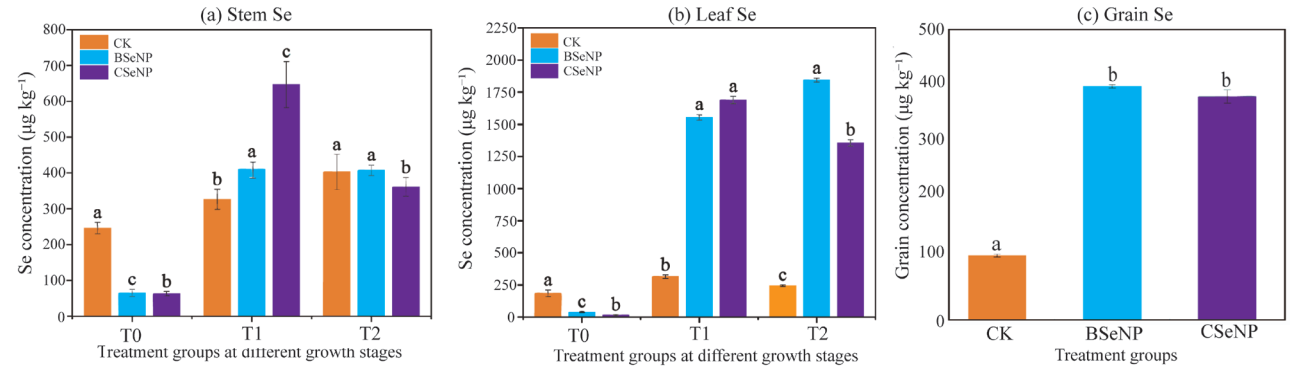

Fig. 4. Selenium accumulation in rice tissues. a) Stem Se content, b) leaf Se content at different growth stages (T0-T2), and c) grain Se content at maturity under CK, BSeNP, and CSeNP treatments. Error bars represent mean±SD (n = 3). Different letters indicate significant differences among treatments ($p<0.05$, one-way ANOVA followed by Tukey's HSD test).

microbiome. This pattern is consistent with earlier reports showing that selenium nanomaterials can influence carbon and nitrogen turnover through selective stimulation of rhizosphere microbial groups.

At the phylum level, Proteobacteria, Actinobacteria, and Acidobacteria remained the dominant bacterial groups, together accounting for >70% of the total sequences (Fig. 5c)). Nano-selenium application significantly increased the relative abundance of Proteobacteria, whereas Actinobacteria declined compared with CK. This shift suggests enrichment of metabolically versatile and stress-tolerant taxa that are commonly associated with nutrient cycling, redox processes, and adaptation to altered microenvironments. Acidobacteria remained an important component of the community but showed comparatively less variation among treatments.

At the genus level, the response to BSeNP and CSeNP differed more clearly. BSeNP preferentially enriched *Burkholderia*, *Rhodobacter*, and *Sphingomonas*, while CSeNP was more strongly associated with *Massilia* and *Ensifer*. These genera are functionally relevant to selenium transformation, antioxidant metabolism, root colonization, and nutrient turnover, indicating that the two nano-selenium formulations did not simply change the same microbial taxa to different degrees, but instead promoted distinct microbial assemblages linked to Se transformation and nutrient cycling.

Co-occurrence network analysis provided additional evidence that nano-selenium altered the organization of the microbial community (Fig. 5(d-f)). Relative to CK, nano-selenium treatments generated more specialized networks characterized by fewer edges and lower overall connectivity. In BSeNP-treated soils, highly connected Rhodobacter and unclassified Burkholderiaceae-affiliated OTUs occupied central network positions and appeared to coordinate selenium transformation and nutrient turnover. In contrast, the CSeNP network incorporated additional associations with *Massilia* and *Ensifer*, indicating a broader but less tightly coupled

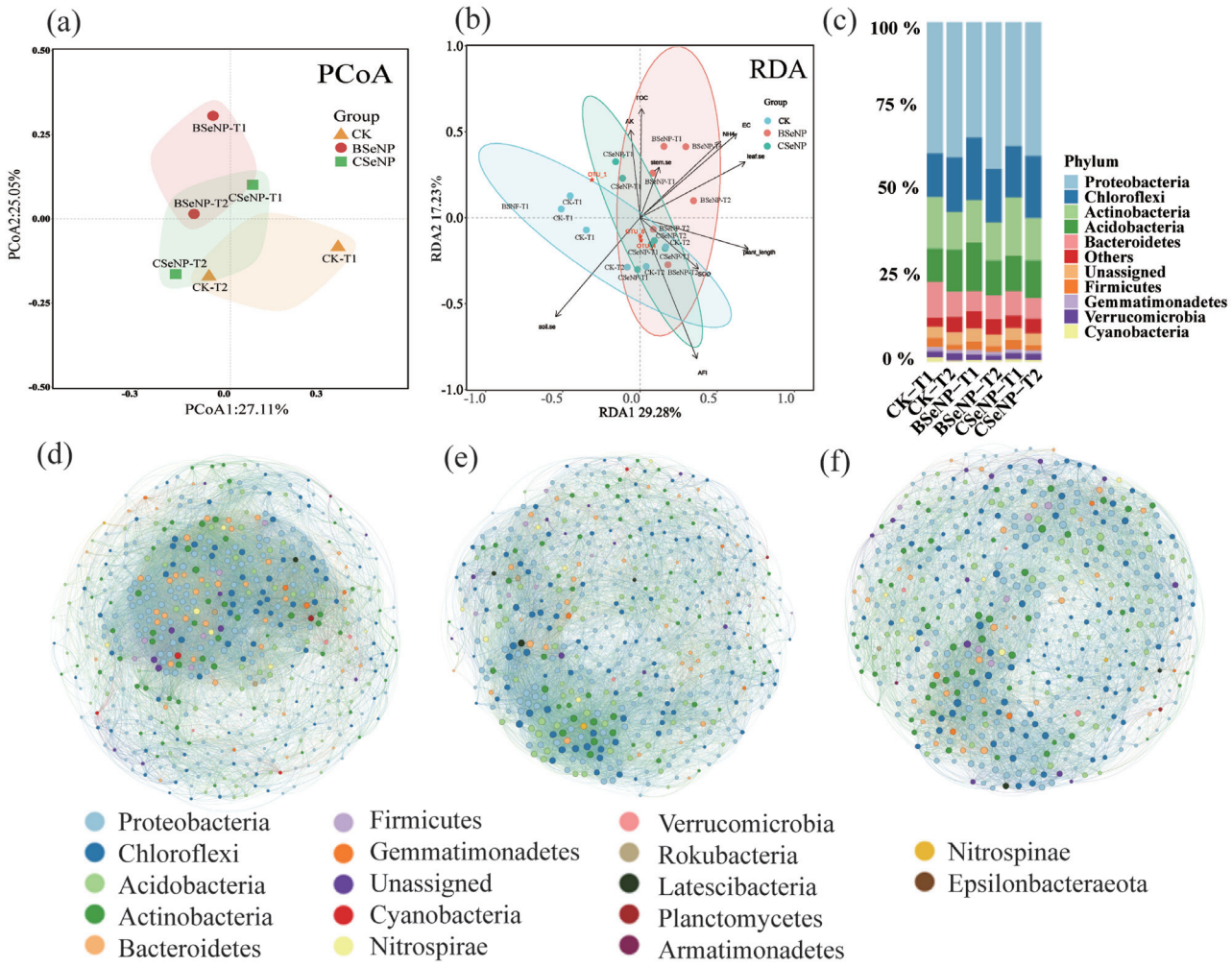

Fig. 5. Microbial community structure and composition. a) Principal coordinate analysis (PCoA) based on microbial community composition. b) Redundancy analysis (RDA) showing relationships between microbial communities and environmental variables. c) Relative abundance of dominant bacterial phyla across treatments and growth stages. (d-f) Co-occurrence networks of microbial communities under CK, BSeNP, and CSeNP treatments, respectively. Nodes represent taxa, and edges indicate significant correlations between taxa. Node colors correspond to different bacterial phyla.

interaction pattern. The higher average node degree and clustering coefficient in BSeNP networks further suggest a more compact and functionally specialized microbial organization than that observed in CSeNP, but lower than that in CK.

Functional Prediction and Microbial–Environmental Correlations

Functional prediction based on KEGG analysis showed that nano-selenium fertilization significantly altered the potential metabolic capabilities of soil microbial communities (Fig. 6a)). Compared with CK, both BSeNP and CSeNP induced pronounced shifts in major pathways, including membrane transport, nitrogen metabolism, sulfur metabolism, and stress response functions. Among these, the BSeNP treatment generally showed the strongest enrichment, indicating a more substantial reorganization of the functional potential of the rhizosphere microbiome.

In particular, the increased abundance of ABC transporter-related functions suggests enhanced microbial transmembrane transport and detoxification capacity under nano-selenium exposure, which may contribute to maintaining selenium homeostasis in the soil microbial community. The enrichment of nitrogen- and sulfur-related pathways indicates strengthened nutrient turnover processes, which are directly relevant to soil fertility and plant growth. These patterns are consistent with previous studies showing that selenium- or biochar-amended soils often exhibit enhanced microbial functions related to nutrient use efficiency and environmental adaptation [17].

FAPROTAX-based functional annotation further corroborated the KEGG results by highlighting ecological functions directly linked to nutrient cycling and environmental adaptability (Fig. 6b)). BSeNP treatment notably increased functions associated with sulfur oxidation, including dark sulfide oxidation, as well as ammonia oxidation and nitrification. These changes indicate that nano-selenium, especially BSeNP,

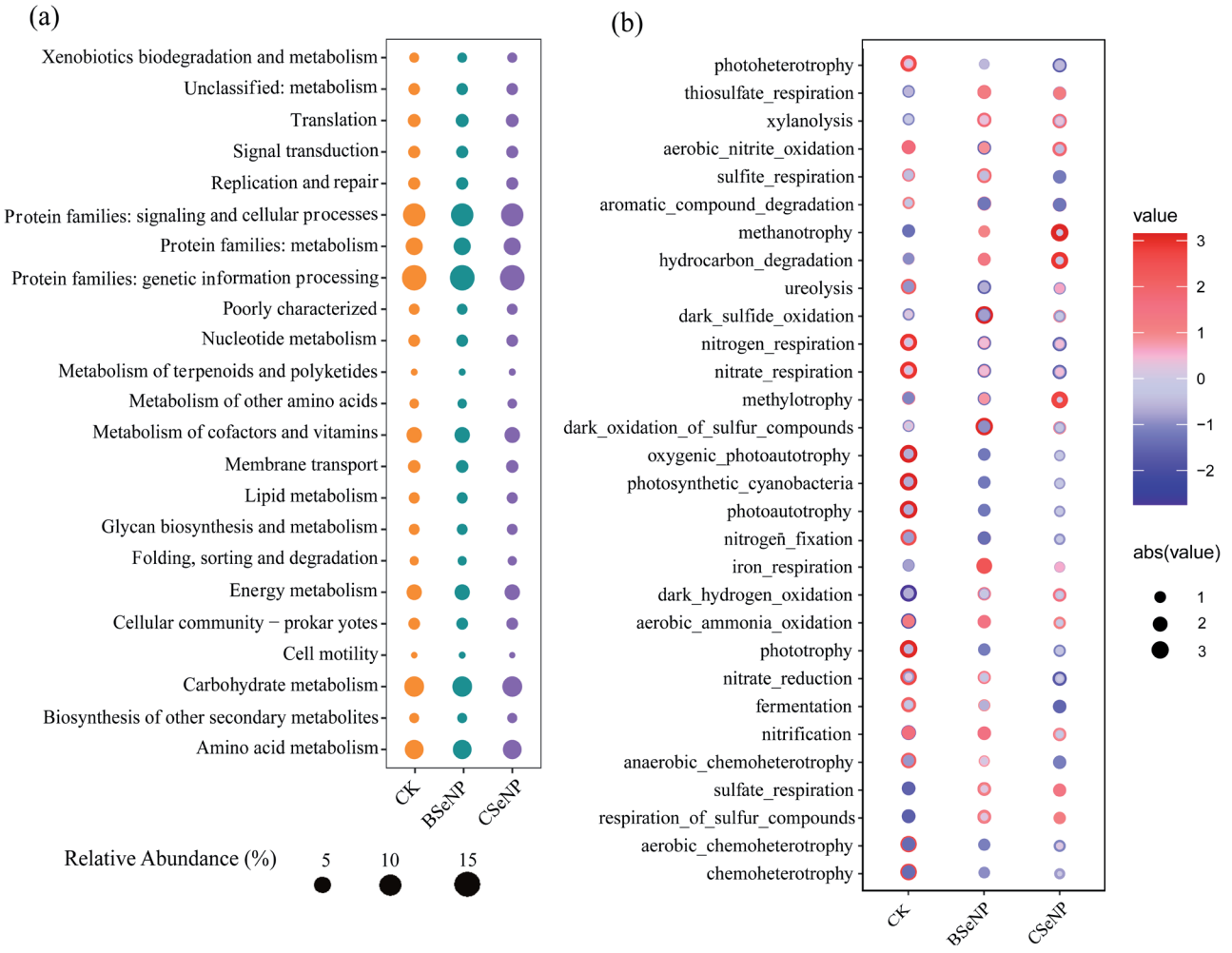

Fig. 6. Functional prediction of microbial communities. a) KEGG functional profiles showing the relative abundance (%) of major metabolic pathways across treatments. Circle size represents the relative abundance of each pathway. b) FAPROTAX-based functional annotation illustrating ecological functional shifts among treatments. Color indicates standardized relative change (Z-score), and circle size represents the magnitude of change.

promoted microbial-mediated nutrient transformation processes that may enhance soil nitrogen and sulfur availability. The strengthened nitrogen-cycling functions under BSeNP also imply the potential for reduced nitrogen loss through denitrification-related pathways, which is consistent with the observed enhancement of Se accumulation and plant performance.

Mantel and Pearson correlation analyses further integrated microbial functional variation with soil physicochemical parameters and plant traits (Fig. 7). In CK soils, correlations were mainly observed between microbial diversity metrics and soil pH and electrical conductivity (EC), indicating a relatively stable but nutrient-limited background condition. Under BSeNP treatment, however, stronger positive associations emerged among microbial community composition, soil nutrients (NH_4^+, NO_3^-, and available K), and plant Se content. Notably, ammonium nitrogen showed a significant correlation with Se accumulation in grains, highlighting the importance of microbial-mediated nutrient transformation for promoting Se uptake and translocation in rice.

Overall, the functional prediction and correlation analyses indicate that nano-selenium fertilization, particularly BSeNP, reshaped soil microbial metabolism toward enhanced nutrient cycling, redox regulation, and selenium bioavailability. These functional shifts, together with the compositional and network-level changes described above, support the existence of strengthened soil–plant–microbe interactions under BSeNP treatment and provide a mechanistic basis for its superior performance in paddy Se biofortification systems.

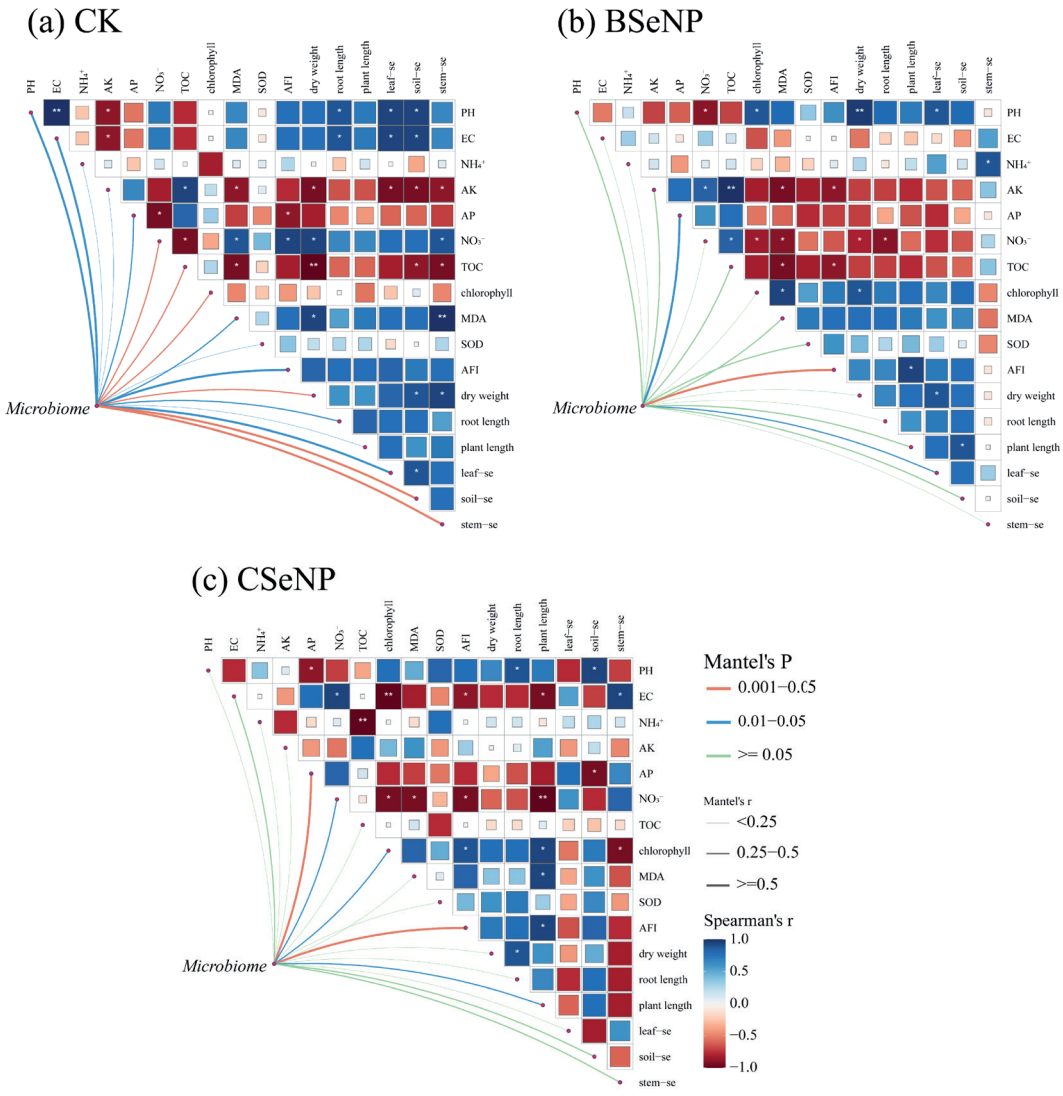

Fig. 7. Relationships among microbial communities, environmental factors, and plant traits. (a-c) Mantel test and Spearman correlation analyses for CK, BSeNP, and CSeNP treatments, respectively. Heatmaps represent Spearman's correlation coefficients (r) among soil physicochemical properties, plant physiological traits, and selenium accumulation variables. Color indicates correlation direction and strength (red, positive; blue, negative). Mantel test results are shown as connecting lines between the microbiome and measured variables, where line color represents significance level (p value) and line width indicates correlation strength (Mantel's r).

Discussion

Nano-Selenium Enhances Se Availability and Biofortification in Rice Systems

The physicochemical characterization of BSeNP and CSeNP demonstrated that the two nano-selenium fertilizers used in the field experiment differed not only in mean particle size and zeta potential, but also in size-distribution patterns, surface morphology, and surface functional-group signatures. Specifically, CSeNP showed a more concentrated particle-size distribution and more uniform SEM morphology, whereas BSeNP exhibited a broader distribution pattern and a distinct biologically mediated surface chemistry.

The continuous decline in soil selenium content, accompanied by sustained increases in plant Se accumulation, suggests that nano-selenium fertilizers effectively improved Se bioavailability and subsequent uptake by rice. This trend indicates that SeNPs dissolve gradually and provide a stable source of bioavailable Se, allowing continuous absorption throughout the crop growth period. In contrast to ionic selenite, which may undergo rapid fixation in paddy soils or volatilization loss, nano-Se forms maintain prolonged root–soil contact and a controlled release, thereby improving uptake efficiency and internal translocation [18].

Both nano-selenium formulations significantly enhanced Se concentrations in stems, leaves, and grains relative to the control. BSeNP showed stronger effects in vegetative tissues, while differences in grain Se were not statistically significant. These physicochemical advantages facilitate direct root interception and membrane transport, promoting Se translocation within plant tissues and redistribution from vegetative organs to grains [19-21]. Significant differences were observed in leaf selenium accumulation between BSeNP and CSeNP treatments, whereas grain Se content showed no statistically significant variation. This pattern may partly stem from the markedly distinct physicochemical properties of the two selenium nanoparticles. BSeNP exhibited a smaller hydrodynamic particle size and higher absolute zeta potential values than CSeNP, indicating superior colloidal stability. Furthermore, SEM and FTIR analyses revealed distinct differences in particle morphology and surface functional group environments between the two formulations. Since leaves are directly exposed to foliar sprays, these formulation-specific variations may be more readily reflected in leaf selenium accumulation, while grain selenium accumulation depends on subsequent redistribution within nutritive tissues during the grain-filling stage, including phloem loading, long-distance transport, and energy-dependent regulation. These processes likely buffered initial differences in leaves, resulting in relatively similar final grain selenium concentrations [22].

Such findings support previous research demonstrating that nano-selenium can improve micronutrient uptake efficiency, enhance antioxidant metabolism, and promote grain nutritional fortification in cereals and leafy vegetables [23]. Moreover, the stronger enhancement observed in BSeNP than CSeNP implies that the biological synthesis route may confer additional ecological and biochemical advantages, including improved surface reactivity, biocompatibility, and interactions with soil microbial processes that further promote Se mobilization and assimilation [24]. Overall, the results indicate that nano-selenium, especially biosynthesized forms, can act as a highly efficient Se delivery system in rice production, boosting Se availability, sustaining uptake during critical growth phases, and ensuring effective distribution to edible tissues.

Soil Microbial Restructuring Drives Nano-Selenium Efficiency

Nano-selenium fertilization not only increased Se uptake in rice but also significantly restructured the soil microbial community, highlighting a critical biological dimension of Se biofortification. Principal coordinate and redundancy analyses demonstrated clear shifts in microbial composition under BSeNP and CSeNP treatments, with BSeNP exhibiting stronger divergence from the control. These community shifts were closely associated with elevated levels of soil carbon, nitrogen, and potassium, suggesting that nano-selenium promotes a nutrient-enriched microhabitat favorable for active microbial metabolism [25].

A characteristic response to nano-selenium was the enrichment of Proteobacteria, a metabolically versatile phylum widely recognized for its key roles in nutrient cycling, root colonization, and trace element transformation. In contrast, Actinobacteria abundance declined, indicating that selenium inputs selectively favored copiotrophic, stress-tolerant functional groups while reducing oligotrophic decomposers [26]. Within Proteobacteria, genera such as *Burkholderia*, *Rhodobacter*, and *Sphingomonas* increased markedly, consistent with their documented capacities for selenite reduction, antioxidant metabolism, auxin biosynthesis, and promotion of plant nutrient uptake [27]. Co-occurrence network analysis further revealed that BSeNP induced a more compact and functionally specialized microbial network relative to CSeNP, cwith more edges and higher mean degree and clustering than CSeNP.

These microbial adjustments correspond well with the observed improvements in plant Se enrichment, implying that nano-selenium strengthens plant-microbe interactions that systemically enhance Se mobilization, transformation, and root uptake [28]. Taken together, the results underscore that nano-selenium efficiency extends beyond direct plant physiological effects and is driven substantially by rhizosphere microbial restructuring, a process especially pronounced under biosynthesized SeNPs [29]. This biological coupling represents a key

mechanism enabling sustainable selenium nutrition and improved ecosystem performance in rice paddy systems.

Collectively, these results demonstrate that nano-selenium fertilizers promote beneficial restructuring of soil microbial communities, characterized by Proteobacteria-enriched, functionally active, and stress-resilient assemblages. Such community reorganization likely enhances nutrient turnover and selenium bioavailability in rice rhizospheres, thereby supporting both soil health and crop selenium fortification.

Nano-Selenium Enhances Functional Pathways for Nutrient Cycling and Redox Regulation

Functional prediction analyses indicated that nano-selenium fertilization not only restructured microbial community composition but also strengthened metabolic pathways associated with nutrient cycling and redox adaptation, particularly under BSeNP treatment. KEGG enrichment revealed significant activation of ABC transporters, nitrogen metabolism, sulfur metabolism, amino acid turnover, and DNA-repair functions, implying that microorganisms experienced enhanced metabolic demand and stress-adaptive responses in nano-selenium environments [30]. These pathways are fundamental to maintaining trace-element homeostasis and cellular redox balance, enabling microbes to tolerate and transform Se species more efficiently [31].

Both BSeNP and CSeNP increased ABC transporter activity, the major transmembrane system mediating selenite/selenate uptake and efflux, supporting the notion that rhizosphere microbes actively participate in selenium detoxification and mobilization [13]. Functional profiles also showed enrichment of nitrification, ammonia oxidation, and sulfur oxidation functions, aligning with reports that selenium nanomaterials stimulate microbial groups involved in oxidative nitrogen turnover and sulfur-linked electron transfer [32]. Differences between formulations were also evident: BSeNP markedly promoted biosynthetic and energy-yielding functions, indicating a more active, growth-oriented microbial consortium, while CSeNP induced pathways associated with oxidative stress mitigation and denitrification, consistent with a more conservative, stress-buffering strategy [33]. These functional contrasts correspond with network results showing a more specialized microbial structure under BSeNP and a diffuse but stress-tolerant assemblage under CSeNP.

Collectively, these results demonstrate that nano-selenium reinforces soil nutrient cycling and redox resilience by stimulating key microbial metabolic functions. Such enhanced biogeochemical activity is likely pivotal for sustaining Se mobilization, supporting plant antioxidative defense, and maintaining soil ecological stability. Compared with chemically synthesized SeNPs, BseNPs showed distinct physicochemical characteristics, stronger effects on microbial network organization, and enhanced enrichment of nutrient-cycling-related functional pathways. These system-level responses suggest that biosynthesized SeNPs offer broader ecological advantages beyond grain Se accumulation, particularly in regulating microbial interactions and nutrient cycling processes.

Coupled Plant-Soil-Microbe Feedbacks Underpin Nano-Selenium Sustainability

The integrated effects of nano-selenium application on rice performance and soil microbial ecology suggest the existence of a coordinated feedback mechanism that enhances nutrient acquisition, redox balance, and selenium cycling in paddy systems [34, 35]. Under BSeNP treatment, strong positive correlations were observed among soil ammonium, available potassium, rice Se content, chlorophyll levels, and antioxidant enzyme activity, indicating that selenium nanoparticles modulated rhizosphere conditions in ways that jointly benefited microbial metabolism and plant physiological performance [18]. The strengthening of these plant–microbe interactions further suggests that nano-selenium altered the biochemical environment surrounding roots, thereby facilitating more efficient nutrient exchange and improved stress adaptation [36].

The nodal dominance of keystone rhizobacteria, including *Burkholderia*, *Rhodobacter*, *Sphingomonas*, and *Ensifer*, further indicates that microbially mediated Se redox transformation and nutrient cycling were closely linked to the efficacy of nano-selenium in flooded soils [27]. Their enrichment under BSeNP suggests a more eco-compatible stimulation of beneficial microbial guilds, which may enhance system efficiency and resilience without favoring undesirable taxa [37].

Overall, these results suggest that nano-selenium application supports a tightly connected plant–soil–microbe interaction network, strengthening the biogeochemical feedbacks required for sustainable Se enrichment and soil health. By stimulating microbial nutrient-cycling pathways and coordinating oxidative regulation in rice, BSeNP in particular may provide a stronger basis for long-term Se biofortification strategies with relatively limited ecological disturbance.

Conclusions

This study demonstrates that biosynthesized nano-selenium (BSeNP) represents a highly promising and ecologically compatible strategy for enhancing selenium biofortification and supporting soil ecological functions in paddy ecosystems. Compared with chemically synthesized nano-selenium (CSeNP), BSeNP exhibited superior Se assimilation efficiency, leading to higher Se accumulation in rice grains and vegetative tissues, as well as more rapid and efficient Se transformation from soil to plant pools. These results confirm the high

bioavailability, controlled release, and effective mobility of nano-selenium in submerged soil–plant systems.

Nano-selenium application substantially reshaped soil microbial communities, characterized by increased abundance of Proteobacteria and enrichment of functional taxa involved in selenium transformation, antioxidant metabolism, and nutrient cycling. BSeNP promoted more a more connected microbial network than CSeNP, containing several highly connected taxa, indicating that biosynthesized nanoparticles can more effectively stimulate beneficial rhizosphere microbiota than their chemically derived counterparts.

Functional prediction analyses revealed that nano-selenium enhanced microbial pathways associated with membrane transport (e.g., ABC transporters), nitrogen and sulfur cycling, amino acid metabolism, and redox regulation, collectively strengthening soil nutrient turnover and improving plant nutrient availability. The strong correlations among microbial metabolic activity, soil NH_4^+ and available K, plant antioxidant traits, and Se accumulation highlight a coordinated soil–plant–microbe feedback mechanism under BSeNP treatment.

Taken together, these findings indicate that biosynthesized nano-selenium enhances Se biofortification while simultaneously promoting soil microbial activity, ecological nutrient cycling, and functional stability. This underscores its potential as a sustainable and high-efficiency alternative to conventional Se fertilizers in flooded agroecosystems. Future studies should address long-term ecological safety, nanoparticle transformation dynamics in paddy soils, and optimized field application rates to maximize agronomic benefits while maintaining microbial and environmental integrity.

Acknowledgments

This study was financially supported by CAS Key Laboratory of Forest Ecology and Silviculture, Institute of Applied Ecology, Chinese Academy of Sciences (No. KLFES-2034) and the Liaoning Provincial Natural Science Foundation of China (2023-BS-024).

AI Usage Disclosure Statement

During the preparation of this manuscript, the authors used OpenAI ChatGPT (web-based interface) solely to assist with English-language editing, sentence restructuring, improvement of readability, and consistency of terminology in text originally prepared by the authors. AI assistance was applied only during manuscript writing and revision.

The tool was not used for study design, literature evaluation, experimental work, data collection, data generation, statistical or bioinformatic analyses, figure preparation, or formulation of scientific conclusions. All AI-assisted text was carefully reviewed, revised, and verified by the authors, who take full responsibility for the accuracy, integrity, and originality of the manuscript.

Conflict of Interest

The authors declare no conflict of interest.

References

1. FAIRWEATHER-TAIT S.J., BAO Y., BROADLEY M.R., COLLINGS R., FORD D., HESKETH J.E., HURST R. Selenium in human health and disease. *Antioxidants & Redox Signaling*, **14** (7), **1337**, **2011**.
2. YANG C., YAO H., WU Y., SUN G., YANG W., LI Z., SHANG L. Status and risks of selenium deficiency in a traditional selenium-deficient area in Northeast China. Science of The Total Environment, **762**, 144103, **2021**.
3. DE LIMA A.B., DE ANDRADE VILALTA T., LESSA J.H.L., LOPES G., GUILHERME L.R.G., GUERRA M.B.B. Selenium bioaccessibility in rice grains biofortified via soil or foliar application of inorganic Se. Journal of Food Composition and Analysis, **124**, 105652, **2023**.
4. ALSHAAL T., SZABOLCSY É.D., FÁRI M., VERES S., KASZÁS L., KOVÁCS Z., EISSA F., ELHAWAT N. Agricultural sustainability and the challenges of selenium nanoparticles (SeNPs): Their role in supporting the environmental economy. Plant Stress, **16**, 100846, **2025**.
5. MRIDHA D., LAMSAL B., ANTONANGELO J.A. Nanotechnology in agriculture: Innovations for sustainability and greenhouse gas mitigation – A review. Science of The Total Environment, **995**, 180065, **2025**.
6. BURMISTROV D.E., SHUMEYKO S.A., SEMENOVA N.A., DOROKHOV A.S., GUDKOV S.V. Selenium nanoparticles (Se NPs) as agents for agriculture crops with multiple activity: A review. Agronomy, **15** (7), 1591, **2025**.
7. KAH M., TUFENKJI N., WHITE J.C. Nano-enabled strategies to enhance crop nutrition and protection. Nature Nanotechnology, **14** (6), 532, **2019**.
8. IQBAL S., BEGUM F., NGUCHU B.A., CLAVER U.P., SHAW P. The invisible architects: microbial communities and their transformative role in soil health and global climate changes. Environmental Microbiome, **20** (1), 36, **2025**.
9. MOULICK D., MUKHERJEE A., DAS A., ROY A., MAJUMDAR A., DHAR A., PATTANAIK B.K., CHOWARDHARA B., GHOSH D., UPADHYAY M.K., YADAV P., HAZRA S., SARKAR S., MAHANTA S., SANTRA S.C., CHOUDHURY S., MAITRA S., MISHRA U.N., BHUTIA K.L., SKALICKY M., OBROČNÍK O., BÁREK V., BRESTIC M., HOSSAIN A. Selenium – An environmentally friendly micronutrient in agroecosystem in the modern era: An overview of 50-year findings. Ecotoxicology and Environmental Safety, **270**, 115832, **2024**.
10. ANURAG Y., KUSUM Y. Exploring the Effect of Engineered Nanomaterials on Soil Microbial Diversity and Functions: A Review. Journal of Environmental Nanotechnology, **13**(1), 48, **2024**.
11. FU R., ZHU M., ZHANG Y., LI J., FENG H. Harnessing the Rhizosphere Microbiome for Selenium Biofortification

in Plants: Mechanisms, Applications and Future Perspectives. Microorganisms, **13** (6), 1234, **2025**.
12. YING S., GUAN Z., OFOEGBU P.C., CLUBB P., RICO C., HE F., HONG J. Green synthesis of nanoparticles: Current developments and limitations. Environmental Technology & Innovation, **26**, 102336, **2022**.
13. NÓBREGA G.N., FERREIRA T.O., ARTUR A.G., DE MENDONÇA E.S., DE O. LEÃO R.A., TEIXEIRA A.S., OTERO X.L. Evaluation of methods for quantifying organic carbon in mangrove soils from semi-arid region. Journal of Soils and Sediments, **15** (2), 282, **2014**.
14. WANG Q., KONG L., HUANG Q., LI H., WAN Y. Uptake and translocation mechanisms of different forms of organic selenium in rice (*Oryza sativa* L.). Frontiers in Plant Science, **13**, 970480, **2022**.
15. SAMYNATHAN R., VENKIDASAMY B., RAMYA K., MUTHURAMALINGAM P., SHIN H., KUMARI P.S., THANGAVEL S., SIVANESAN I. A recent update on the impact of nano-selenium on plant growth, metabolism, and stress tolerance. Plants, **12** (4), 853, **2023**.
16. WANG C., YUE L., CHENG B., CHEN F., ZHAO X., WANG Z., XING B. Mechanisms of growth-promotion and Se-enrichment in *Brassica chinensis* L. by selenium nanomaterials: beneficial rhizosphere microorganisms, nutrient availability, and photosynthesis. Environmental Science: Nano, **9** (1), 302, **2022**.
17. JIANG Z., WANG Z., ZHAO Y., PENG M. Unveiling the vital role of soil microorganisms in selenium cycling: a review. Frontiers in Microbiology, **15**, 1448539, **2024**.
18. ACUÑA J.J., JORQUERA M.A., BARRA P.J., CROWLEY D.E., DE LA LUZ MORA M. Selenobacteria selected from the rhizosphere as a potential tool for Se biofortification of wheat crops. Biology and Fertility of Soils, **49** (2), 175, **2013**.
19. HAN Q., ZHU G., QIU H., LI M., ZHANG J., WU X., XIAO R., ZHANG Y., YANG W., TIAN B., XU L., ZHOU J., LI Y., WANG Y., BAI Y., LI X. Quality traits drive the enrichment of *Massilia* in the rhizosphere to improve soybean oil content. Microbiome, **12** (1), 224, **2024**.
20. BURK R.F., HILL K.E. Regulation of selenium metabolism and transport. Annual Review of Nutrition, **35** (1), 109, **2015**.
21. TANG Z., FENG X., LI R., FAN F., MIAO Z. Mechanisms of biochar in modulating soil organic selenium transformation and enhancing soil selenium availability. Agronomy, **15** (3), 701, **2025**.
22. DENG G., FAN Z., WANG Z., PENG M. Dynamic role of selenium in soil–plant–microbe systems: mechanisms, biofortification, and environmental remediation. Plant and Soil, **515** (2), 1085, **202**.
23. KHAN Z., THOUNAOJAM T.C., CHOWDHURY D., UPADHYAYA H. The role of selenium and nano selenium on physiological responses in plant: a review. Plant Growth Regulation, **100** (2), 409, **2023**.
24. WANG M., DINH Q.T., QI M., WANG M., YANG W., ZHOU F., LIANG D. Radicular and foliar uptake, and xylem- and phloem-mediated transport of selenium in maize (*Zea mays* L.): a comparison of five Se exogenous species. Plant and Soil, **446** (1), 111, **2020**.
25. ISLAM M.S., SAMS S.U., MALITHA S.B., ALAM M.Z. Trend analysis of reaction parameters and properties of plant-mediated green synthesized selenium nanoparticles using non-parametric statistical methods. RSC Advances, **15** (34), 23215, **2025**.
26. DI X., LUO Y., LI S., LIU K., LI C., WANG Z., YANG F., WANG G. Selenium distribution, translocation and speciation in wheat (*Triticum aestivum* L.) after foliar spraying selenite and selenate. Food Chemistry, **404**, 134716, **2023**.
27. HUANG S., HAN Y., SONG R., WANG X., ZHOU Y., LUO H., REN X., YU K. Effects of bio-nano-selenium on wheat grain morphology, selenium transport enrichment and antioxidant enzyme activities. Frontiers in Plant Science, **16**, 1516005, **2025**.
28. QIN X., WANG Z., LAI J., LIANG Y., QIAN K. The synthesis of selenium nanoparticles and their applications in enhancing plant stress resistance: a review. Nanomaterials, **15** (4), 301, **2025**.
29. WANG Y., XUECHONG X., CHEN H., ZHANG K., ZHAO B., QIU R. Selenium-induced enhancement in growth and rhizosphere soil methane oxidation of prickly pear. Plants, **13** (6), 749, **2024**.
30. ZHOU Y., BASTIDA F., LIU Y., LIU Y., XIAO Y., SONG P., WANG T., LI Y. Selenium fertigation with nanobubbles influences soil selenium residual and plant performance by modulation of bacterial community. Journal of Hazardous Materials, **423**, 127114, **2022**.
31. HUSEN A., SIDDIQI K.S. Plants and microbes assisted selenium nanoparticles: characterization and application. Journal of Nanobiotechnology, **12** (1), 28, **2014**.
32. HUSSAIN M., ADEEL M., WHITE J.C. Nano-selenium: a novel candidate for plant microbiome engineering. Trends in Plant Science, **30** (5), 454, **2025**.
33. SUNG K., PARK M., KWEON O., SAVENKA A., PAREDES A., SADAKA M., KHAN S., MIN S., FOLEY S. Species-specific stress responses to selenium nanoparticles in *Pseudomonas aeruginosa* and *Proteus mirabilis*. Nanomaterials, **15** (18), 1404, **2025**.
34. NEDJIMI B. The role of selenium and selenium nanoparticles in enhancing plant tolerance to cadmium stress: a sustainable approach. Discover Plants, **2** (1), 129, **2025**.
35. ESTARRIAGA-NAVARRO S., GOICOECHEA N., PLANO D., SANMARTÍN C. Selenium biofortification: integrating one health and sustainability. Journal of the Science of Food and Agriculture, **106** (4), 1955, **2025**.
36. LUO C., HE Y., CHEN Y. Rhizosphere microbiome regulation: Unlocking the potential for plant growth. Current Research in Microbial Sciences, **8**, 100322, **2025**.
37. WANG C., CHENG B., LI J., LI X., FENG Y., KAH M., YUE L., CAO X., FAN Z., JI Y., WANG Z., XING B. Application of selenium-engineered nanomaterials to paddy soil promote rice production by improving soil health. Communications Earth & Environment, **6** (1), 448, **2025**.